scientific reports

OPEN

Fundus camera-based precision monitoring of blood vitamin A level for Wagyu cattle using deep learning

Nanding Li[1,2,3], Naoshi Kondo[2], Yuichi Ogawa[2], Keiichiro Shiraga[2], Mizuki Shibasaki[2], Daniele Pinna[4], Moriyuki Fukushima[2], Shinichi Nagaoka[2], Tateshi Fujiura[2], Xuehong De[1,3]✉ & Tetsuhito Suzuki[5]✉

In the wagyu industry worldwide, high-quality marbling beef is produced by promoting intramuscular fat deposition during cattle fattening stage through dietary vitamin A control. Thus, however, cattle become susceptible to either vitamin A deficiency or excess state, not only influencing cattle performance and beef quality, but also causing health problems. Researchers have been exploring eye photography monitoring methods for cattle blood vitamin A levels based on the relation between vitamin A and retina colour changes. But previous endeavours cannot realise real-time monitoring and their prediction accuracy still need improvement in a practical sense. This study developed a handheld camera system capable of capturing cattle fundus images and predicting vitamin A levels in real time using deep learning. 4000 fundus images from 50 Japanese Black cattle were used to train and test the prediction algorithms, and the model achieved an average 87%, 83%, and 80% accuracy for three levels of vitamin A deficiency classification (particularly 87% for severe level), demonstrating the effectiveness of camera system in vitamin A deficiency prediction, especially for screening and early warning. More importantly, a new method was exemplified to utilise visualisation heatmap for colour-related DNNs tasks, and it was found that chromatic features extracted from LRP heatmap highlighted-ROI could account for 70% accuracy for the prediction of vitamin A deficiency. This system can assist farmers in blood vitamin A level monitoring and related disease prevention, contributing to precision livestock management and animal well-being in wagyu industry.

Keywords Fundus imaging, Deep learning, Vitamin A estimation, Japanese black cattle, Precision Livestock Farming

List of symbols

DNNs	Deep neural networks
FN	False negative
FP	False positive
HPLC	High-performance liquid chromatography
IMF	Intramuscular fat
I/O	Input/output
IOU	Intersection over union
IU	International unit
LRP	Layer-wise relevance propagation
mAP@0.5	mean average precision, when IOU is at 0.5
mo	Month
n	Pixel number

[1]School of Mechanical and Electrical Engineering, Inner Mongolia Agricultural University, No.306 Zhaowuda Rd, Hohhot, Inner Mongolia Autonomous Region, China. [2]Graduate School of Agriculture, Kyoto University, Kyoto, Japan. [3]Inner Mongolia Engineering Research Center of Intelligent Equipment for the Entire Process of Forage and Feed Production, Hohhot, China. [4]Department of Agricultural Sciences, University of Sassari, Sassari, Italy. [5]Graduate School of Bioresources, Mie University, 1577 Kurimamachiyacho, Tsu, Mie 514-8507, Japan. ✉email: dexuehong2022@imau.edu.cn; t-suzuki@bio.mie-u.ac.jp

PL filter	Polarising filter
PR curve	Precision-recall curve
ROI	Region of interests
R_{ave}, G_{ave}, B_{ave}	Average value of RGB channels
R_i, G_i, B_i	Each pixel value of eye surface or fundus ROI in RGB channels
R_{ratio}, G_{ratio}, B_{ratio}	Red, green, and blue component ratios
$R_{variance}$, $G_{variance}$, $B_{variance}$	Red, green, and blue channels variances
SVM	Support vector machine
TN	True negative
TP	True positive
YOLO	You only look once model

Beef marbling quality is determined by both genetic factor and nutrition factor[1]. Not only in wagyu cattle, but also in Angus and many others, beef marbling is significantly dependent on blood vitamin A[2] levels (Supplementary material Fig. S1) during cattle growth[3–7]. This holds true particularly for Japanese Black cattle – a renowned breed selected for high marbling beef (Supplementary material Fig. S2). A higher level of vitamin A inhibits intramuscular fat (IMF) deposition[8,9], consequently lowering beef quality. Conversely, too low vitamin A concentration (below 30 IU dL^{-1}) leads to hypovitaminosis A, causing night blindness[10], joint oedema[11], liver damage[12,13], and other diseases[14], from which, animals suffer so much. As such, not only a responsible awareness of animal welfare, but also a higher standard of precision livestock requirement in the wagyu husbandry system, necessitate an effective, timely monitoring of blood vitamin A levels.

During the fattening stage, wagyu cattle undergo vitamin A decrease period, resulting in reduced amount of chromophore retinal (vitamin A derivatives). This, in turn, leads to a diminished supply of photopigment (such as rhodopsin) in the retinoid cycle[15], causing fundus colour change from blueish to pale macroscopically (Supplementary material Fig. S3). It is based on this colour changes due to the blood vitamin A levels[16–18], that our team has proposed an ophthalmological and photographical method for non-invasive monitoring of vitamin A condition using eye imaging[19–25], aiming to replace the conventional blood assay method, which is expensive, time consuming, and potentially stressful to cattle.

Deep Neural Networks (DNNs) embraced a boom in a vast variety of tasks nowadays[26,27], including animal applications[28–30]. In human ophthalmology, DNNs have been successfully applied on retinal fundus photographs to detect or classify human eye diseases such as diabetic retinopathy, glaucomatous damages, and others[30–33]. It was the abnormal changes in colour, shape, or size of specific area (including retinal biomarkers and lesions) in retinal fundus image that provided evidence for the automated detection and diagnosis of eye diseases, such as the red colour from the retinal bleeding (haemorrhage)[34,35], irregularities of shape and appearance of the retinal venules (venous beading)[36], pale optic disc or unusual CDR (cup disc ratio)[37,38] etc. However, in the case of cattle eyes, no such abnormality is observed in the retinal fundus during the normal fattening process, regardless of how high (119 IU dL^{-1}) or low (21 IU dL^{-1}, below the critical level) the blood vitamin A level is. Besides, in the classification task of human eye diseases, some targets (diseased area, such as exudates or optic disc) are so distinct from each other or from their surroundings that their classification task poses no challenge to a DNN architecture which already demonstrated persuasive performance in various public datasets. Whereas in our study, all cattle fundi exhibit high similarity, and the only discernible difference in the fundus images associated with varying levels of vitamin A seems to be the moderate changes in fundus colour, which is, by human diagnosis, impossible to correlate with vitamin A condition. These points make the task of fundus image-based cattle vitamin A prediction markedly distinct from and more challenging than human fundus disease classification. Furthermore, though previous studies pioneered the prediction of blood vitamin A levels[19,21,22,24], their device systems need on-site installation, and their methods required a separate image processing procedure, thus making real-time monitoring unattainable. This is not convenient for farmers or relevant industry personnel. More importantly, their overall prediction accuracy still needs improvements in a practical sense. For example, Han et al.[21] obtained 74.8%, 56.6%, and 62.2% accuracy for the three levels of vitamin A deficiency and Zhou et al.[19] found 0.64% R^2 in the multiple linear regression for vitamin A level estimation. There is need for an accurate, fast, affordable, and easily operable methodology for monitoring blood vitamin A condition. We wish to put into application our findings and technology of fundus photography-based vitamin A prediction and dedicate it to a higher level of precision livestock management.

In the present work, we developed a handheld camera system capable of capturing cattle fundus images and predicting blood vitamin A levels in real time using deep learning algorithms.

Methods
Camera
A new handheld fundus camera was conceptualised for realising easy and flexible image acquisition and real-time vitamin A prediction. This camera system mainly consists of a camera (The Imaging Source, DFK23U445), lens (VS Technology, f8mmVS-0818VM), centre LED (NICHIA NVNWS007), ring LED (NICHIA NSDW570G-Kl), half mirror, polarising filters (PL filters) and a tablet computer (Microsoft Surface Go2). Interior structure of the system and its photography light path was illustrated in Fig. 1.

The core light path lies in the polarised illuminating system. Light from centre LED was polarised by a PL filter and directed towards the eye. A portion of it reached the eye surface and the others went through the pupil onto the retina. Specular reflection occurred at the eye surface and the reflected light was suppressed by another perpendicularly oriented PL filter arranged in front of the camera. Thus, the pupil reflection was eliminated in the fundus image. By contrast, diffuse reflection occurred at the retina and only those of the same direction components with PL filter (camera side) could pass it, while other diffuse reflection was suppressed likewise.

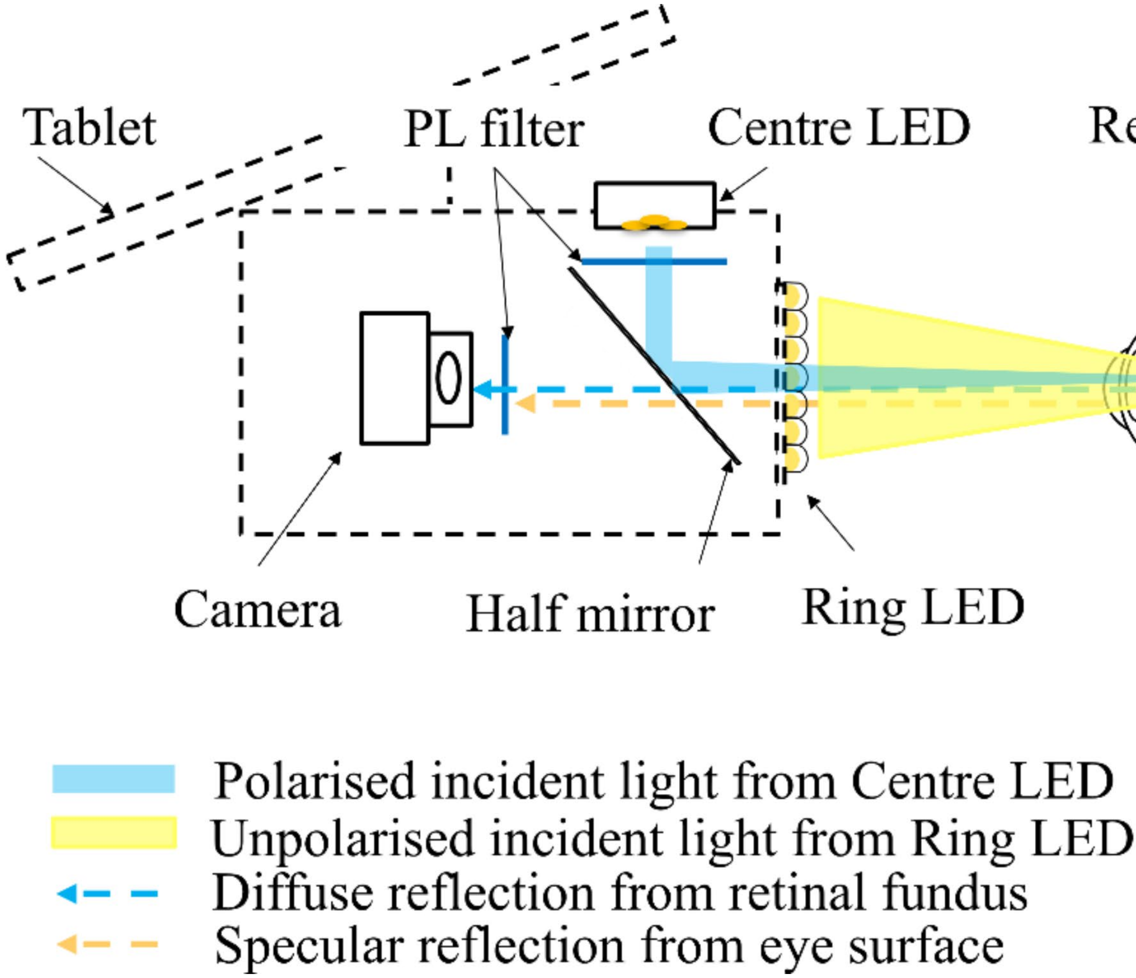

Fig. 1. Interior structure of the fundus camera system and the light path.

Thus, the interior retinal fundus was clearly observed. Taking into consideration the need for enough object illumination as well as reducing ocular stress for cattle, the LED illuminous intensity was set to 1200 lx. The tablet functions as I/O unit as well as storage.

Animal experiment

Fifty clinically healthy Japanese Black cattle were tested in the photographic experiment at the collaborative farm of Tajima Agricultural High School, Hyogo Prefecture, Japan. To explore the potential of fundus-based vitamin A prediction across a broader range of animal group, steers from early, middle, and late fattening stages were all included in this experiment, just like a typical cattle farm. Their monthly ages spanned from 8 ~ 32 mo. To describe the experimental process concisely, the above-mentioned handheld camera was used to take fundus images of both right and left eye from each cattle (Fig. 2a). Then, blood collection was conducted via jugular venepuncture and vitamin A concentration measured by high-performance liquid chromatography (HPLC) in the Hoken Kagaku laboratory, Japan (Health Science Research Institute). In this way, the photographic experiment was performed every two months and continued for 10 months overall. Animal experiment approval was obtained from the Management Office for Research Regulations, Kyoto University, and the experiments are subject to Regulations on Animal Experimentations at Kyoto University. All methods are reported in accordance with ARRIVE guidelines.

YOLO model and statistical analysis

In this study, the most basic model in YOLO 5 family, v5s model, was used to detect and classify the fundus images. It is favoured in a wide range of industrial applications for its good balance of efficiency, accuracy, and computational economy. The model was trained on a desktop PC with 32 batch size and 210 epochs (specifications: CPU Core i7-8700,3.2 GHz; GPU RTX 2080 Super; RAM 32G; OS Windows 10 edu; Python 3.7.6; Pytorch 1.5.0; CUDA 10.2.89; cuDNN 7.6.5). As several images were available for each session (see *3.1. Handheld camera and fundus image* section), it was split randomly at the session level into training (70%) and test (30%) set. This is crucial to avoid data from the same session being present in both training and test samples and to ensure the evaluation accountability.

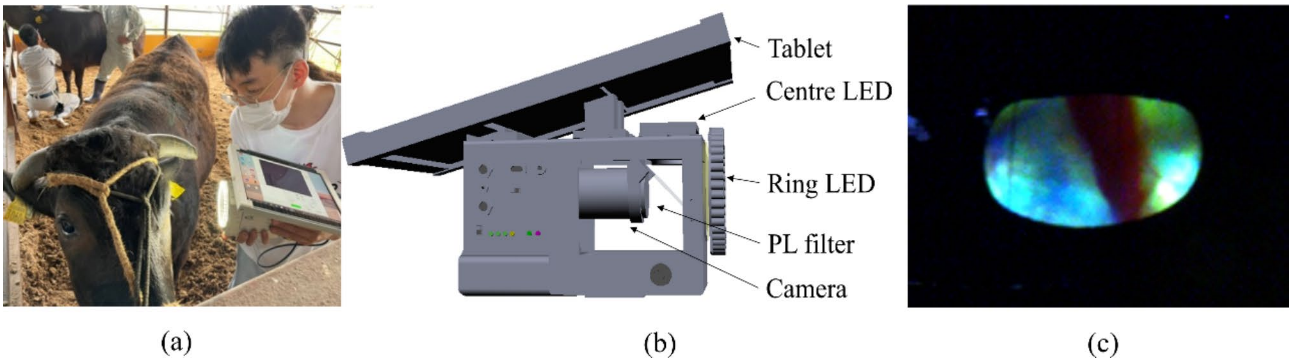

Fig. 2. A handheld fundus camera: (**a**) easy use in taking fundus images; (**b**) main components and model structure; (**c**) an example of cattle fundus image. (identifiable information/image see Informed consent).

Although being effective in enhancing system's robustness, synthetic image or data augmentation technique was not adopted in this study. Obviously, the detection of fundus is intrinsically associated to colour features of retina. What is desired is to input into the model images with their original information, rather than contrast-enhanced or colour-modified images. On the other hand, considering the unbalanced sample data for vitamin A deficiency levels, the effect of non-colour related augmentation was investigated (see *3.2. Vitamin A deficiency classification and data characterisation*).

Statistical analysis was conducted to evaluated YOLO model's performance by a variety of metrics, including TP (true positive), TN (true negative), FP (false positive), FN (false negative), precision, recall, mean average precision (mAP@0.5, when IOU is at 0.5), accuracy, as well as confusion matrix. F1-score and PR curve (precision-recall) were also presented, considering the class-imbalance problem. 3-fold cross validation was implemented for assessing the model and to ensure the generalisation ability on the whole datasets.

LRP heatmap

Layer-wise Relevance Propagation[39,40] is an algorithm that can trace the contribution to the final classification back to the input layer by layer and visualises the relevance/importance of each pixel in heatmaps. Its core idea is to decompose the prediction $f(\mathrm{x})$ as the sum of terms of separate input pixel x_{d}. as shown in the Eq. (1).

$$\mathrm{f}\left(\mathrm{x}\right)=\sum_{d=1}^{V}R_{d} \tag{1}$$

where R_{d} is the relevance score, with $R_{\mathrm{d}}>0$ representing the presence of the target structure while $R_{\mathrm{d}}<0$ representing the absence. $V$is the dimensionality. Considering the fact of almost identical fundus images except for colours in this study, LRP fits this fundus classification task better for both class-discriminative and fine-grained visualising ability, as compared to other methods, such as Guided Backpropagation or Grad-CAM[41–43] etc.

Chromatic feature extraction

Following the LRP heatmap generation, in total, 21 chromatic features were extracted from heatmap-highlighted ROI. They were the average, ratio, and variance of each channel in the RGB space, average and variance of each channel in HSV and Lab colour spaces:

$$\left(R_{\mathrm{ave}},G_{\mathrm{ave}},B_{\mathrm{ave}}\right)=\left(\frac{\sum_{i=1}^{n}R_{i}}{n},\frac{\sum_{i=1}^{n}G_{i}}{n},\frac{\sum_{i=1}^{n}B_{i}}{n}\right) \tag{2}$$

$$\left(R_{\mathrm{ratio}},G_{\mathrm{ratio}},B_{\mathrm{ratio}}\right)=\left(\frac{\sum_{\mathrm{i}=1}^{\mathrm{n}}\left(\mathrm{R_{i}}-\mathrm{R}\right)^{2}}{\mathrm{n}},\frac{\sum_{i=1}^{n}\left(G_{i}-G\right)^{2}}{n},\frac{\sum_{i=1}^{n}\left(B_{\mathrm{i}}-B\right)^{2}}{n}\right) \tag{3}$$

$$\left(R_{\mathrm{var}},G_{\mathrm{var}},B_{\mathrm{var}}\right)=\left(\frac{\sum_{\mathrm{i}=1}^{\mathrm{n}}\left(\mathrm{R_{i}}-\mathrm{R}\right)^{2}}{\mathrm{n}},\frac{\sum_{i=1}^{n}\left(G_{i}-G\right)^{2}}{n},\frac{\sum_{i=1}^{n}\left(B_{\mathrm{i}}-B\right)^{2}}{n}\right) \tag{4}$$

where, n is the pixel number, Ri, Gi, and Bi are each pixel value of fundus ROI in RGB channels respectively; R_{ave}, G_{ave}, and B_{ave} are the average value of red, green, and blue channel; R_{ratio}, G_{ratio}, and B_{ratio} are red, green, and blue component ratios while R_{var}, G_{var}, and B_{var} are the counterpart variances respectively.

HSB and Lab colour spaces are converted from RGB space according to the OpenCV documents. Then average value and variance are calculated likewise (see Supplementary Note).

Results

Handheld camera and fundus image

In this study, we developed a handheld fundus camera for image acquisition and real-time vitamin A prediction. In comparison to the stationary camera system in our preceding research[24]: (1) this is compact, lightweight, and unrestricted to the photography time or farm facility limitations. It is designed specifically for a demand of easier operation and improved flexibility. Furthermore, (2) it integrated a tablet computer deployed with DNNs to realise the real-time prediction. As shown in Fig. 2a, it captures fundus images (in the vicinity of cattle eyes) with a simple click of button. Such a shooting captures one session of 10 consecutive images (10 fps, 1280 × 960, BMP file, 32bit). Figure 2b. shows the main components of this camera model. A combined illuminating systems consisting of a centre LED and ring LED as well as the polarising filters (PL filter) effectively eliminates the specular reflection at the eye surface (Fig. 1) and enables the interior retinal fundus (Fig. 2c) to be observed.

Vitamin A deficiency classification and data characterisation

In total, 4000 fundus images were collected from 50 cattle during their fattening period in the eye photography experiment. Blood vitamin A concentration corresponding to each fundus image was also obtained. The overall vitamin A ranged from 21 ~ 119 IU dL^{-1}, with age spanning from 8 ~ 32 mo across their fattening stage. Considering the normal blood vitamin A fluctuation arising from individual differences in vitamin A tolerance among cattle, a direct prediction of blood vitamin A concentration could be too exacting and also unnecessary for farmers. Therefore, in this study, the vitamin A prediction was implemented as classification task of vitamin A deficiency level[21] to balance between the prediction accuracy and robustness. The fundus images were grouped (according to the Japanese wagyu fattening guideline) into three vitamin A deficiency levels: mild (67–100 IU dL^{-1}), moderate (34–66 IU dL^{-1}), and severe (0–33 IU dL^{-1}), as shown in Table 1. It is clear the sample numbers are unbalanced, particularly for the severe class. However, this is consistent with the real farm situation where cattle experience a low vitamin A fattening for a short period. These images were used for the algorithm training and testing with a YOLO[44] architecture. On the other hand, non-colour related augmentation method (rotation, 0 to 45 degree) was adopted for enlarging the severe class data and the analysis results were presented in the discussion part (see *4. Discussion*).

YOLO performance

Example of fundus images from three vitamin A deficiency levels and their respective YOLO predictions are shown in Fig. 3. For assessing model's generalisation ability, 3-fold cross validation was implemented (Supplementary material table S2-1, S2-2, S2-3), and the prediction results, as detailed in Table 2, show YOLO model achieved an average mAP@0.5 of 0.81, 0.85, and 0.87 in three folds respectively for the three vitamin deficiency classes while their corresponding accuracy reached 0.83, 0.80, and 0.88. The average classification metrics for the three levels are presented in Table 3. To address the problem of unbalanced sample number for each class, precision-recall (PR) curve is generated to reflect the prediction performance more objectively. A confusion matrix for classification is also presented (Fig. 4). Details of other evaluation metrics, such as true positive (TP), false positive (FP), true negative (TN), and false negative (FN), for each class are provided in the Supplementary material table S3-1, S3-2, S3-3.

The classification of vitamin A deficiency levels exhibited encouraging performance. This suggests that specific area in the fundus image could be "detected", and this very ROI is closely related with blood vitamin A concentration. However, the intrinsic "black box" functionality of DNNs could not provide more explanation to such outcomes.

Heatmaps and colour feature-based classification

To better understand the input (fundus image)'s relevance to the output (vitamin A level) class, the Layer-wise Relevance Propagation (LRP), a class decision heatmapping technique, was conducted to localise the ROI in fundus area (see supplementary material Fig. S4). Then, different from all other studies that stopped at this step merely showing the heatmap, this study extracted chromatic features from these ROIs to predict blood vitamin A conditions. By this means, we can not only verify if the ROIs are viable to reflect the retinal chromatic features in cattle eye, but can also explain, in the context of fundus images, how much of the YOLO vitamin A prediction is associated with fundus chromatic features. Figure 3 (third column) shows the LRP heatmaps of the retinal fundus images. Using them as masks, 21 handcraft chromatic features were extracted from the fundus images for vitamin A deficiency classification. The mean and standard deviation of the features are presented in supplementary material table S4-1. The SVM was used for this analysis since it is one of the most powerful machine learning algorithms for classification problem, and, to compare directly with our prior work that used the SVM. Classification results are presented in Table 4.

Datasets*	Fundus No.			Label No.
	Early[a]	Middle[a]	Late[a]	
mild	604	878	134	1616
moderate	103	1196	675	1974
severe	0	130	280	410

Table 1. Summary of datasets. *Cattle gender is steer. Heifers and production cows were not used. [a] "Early", "Middle", and "Late" represent three fattening stages of cattle.

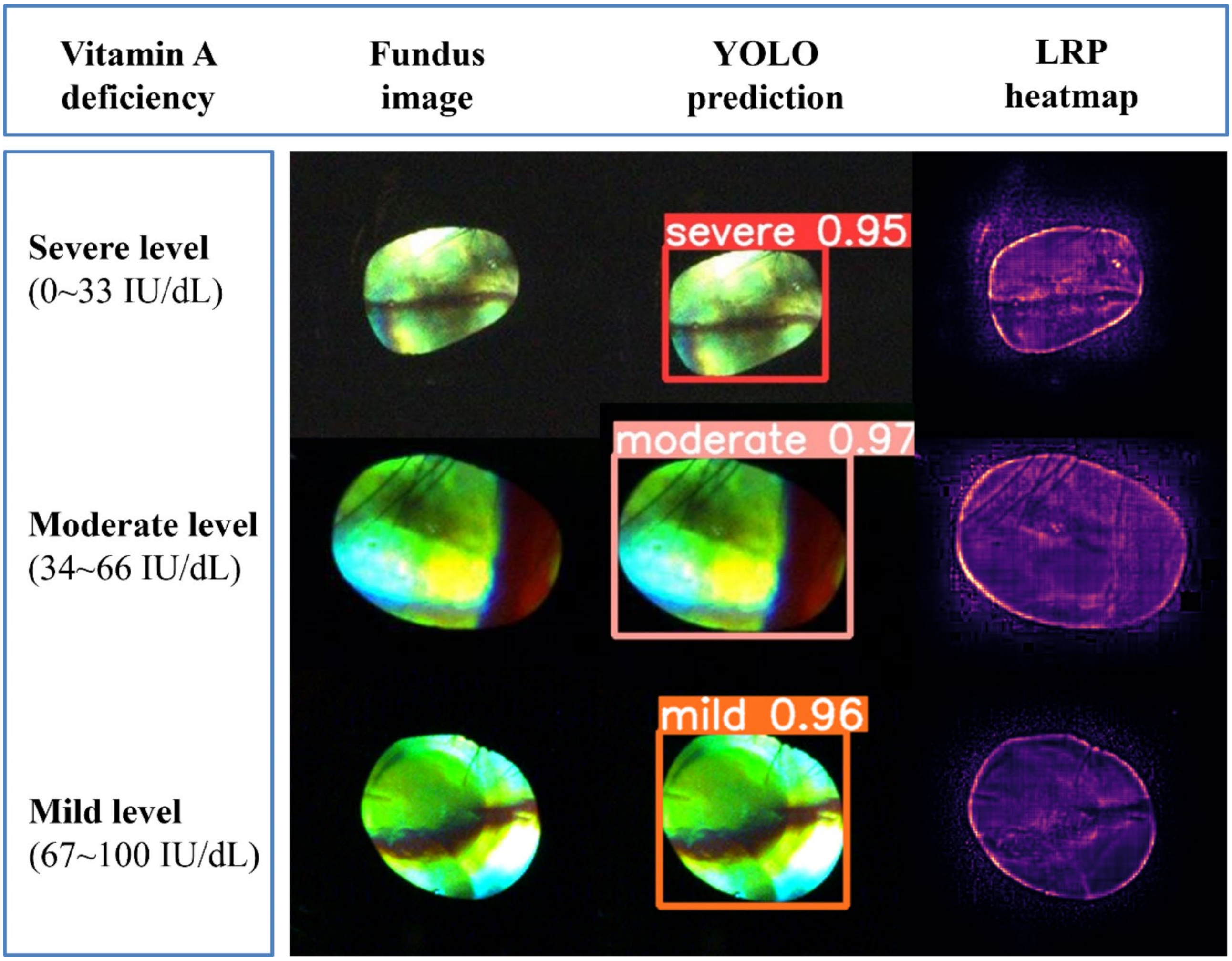

Fig. 3. Example of YOLO predictions for fundus images as well as corresponding LRP heatmaps. The first column: typical cattle fundus images for three vitamin A deficiency levels. Second column: their YOLO prediction results. Third column: fundus LRP heatmaps highlighted for vitamin A predictions.

Fold	Precision	Recall	F1	mAP@0.5	Accuracy
1	0.7	0.81	0.75	0.81	0.83
2	0.78	0.81	0.79	0.85	0.80
3	0.83	0.80	0.81	0.87	0.88

Table 2. 3-fold cross validation on all datasets.

Class	Precision	Recall (Sensitivity)	Specificity	F1	Accuracy
Severe	0.79	0.88	0.97	0.83	0.87
Moderate	0.78	0.77	0.78	0.77	0.83
Mild	0.74	0.78	0.76	0.76	0.80

Table 3. Mean classification metrics for vitamin A deficiency states using YOLO.

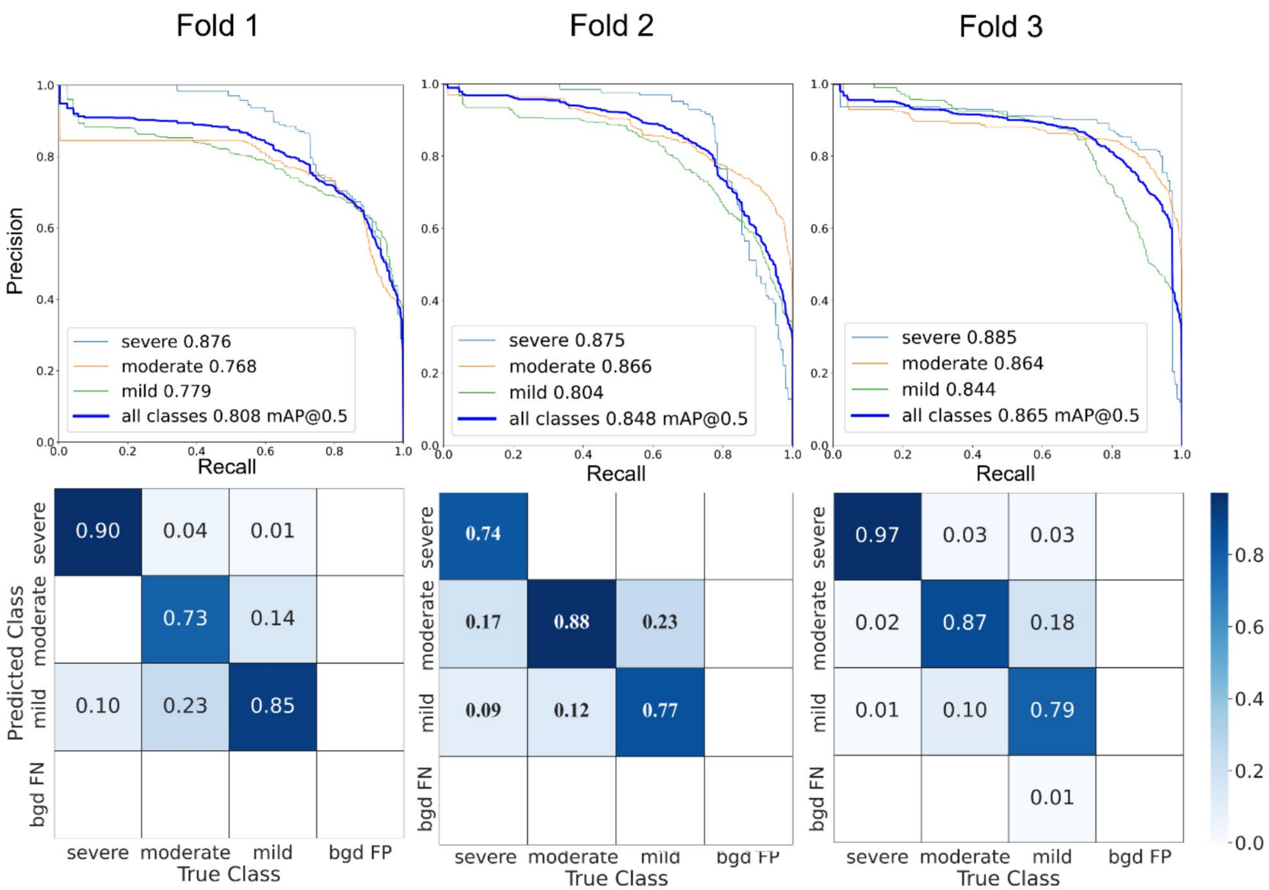

Fig. 4. Classification performance for vitamin A deficiency. PR curve and confusion matrix were generated for each fold to assess the model's performance and reflect the generalisation ability on the whole datasets.

Class	Precision	Recall (Sensitivity)	Specificity	F1	Accuracy
Severe	0.63	0.74	0.96	0.68	
Moderate	0.72	0.78	0.68	0.75	0.70
Mild	0.68	0.60	0.82	0.64	

Table 4. SVM classification metrics for vitamin A deficiency states based on handcraft chromatic features.

As is clear from the comparison between Tables 3 and 4, the YOLO classification yielded 87%, 83%, and 80% of accuracy for severe, moderate, and mild classes, while the chromatic features accounted for an averaged 70% in the SVM prediction.

Deployment in camera system

The YOLO model was trained on desktop PC and then deployed in the fundus camera system, as shown in Fig. 5. The captured images can be examined through the display window before being saved with cattle ID together. After the fundus image collection, a program would direct to the DNNs prediction and yield results.

Discussion

To authors' knowledge, this is the first report about real-time monitoring for cattle vitamin A deficiency levels using deep learning algorithms in retinal fundus photography. Previously, Han et al.[21] obtained 62%, 57%, and 75% classification accuracy for the severe, moderate, and mild group respectively, as shown in Table 5. However, their device can only capture the eye surface image rather than the retinal fundus itself. This hinders more accurate vitamin A prediction — fundus image can more truthfully reflect the retina colour than eye surface image. Then the innovation of double imaging camera system in our preceding research[24] enabled both eye surface and fundus photography. Their corresponding overall classification accuracy reached 76% and 82% respectively. Although the prediction performance improved, the requirements for the imaging system installation on farm

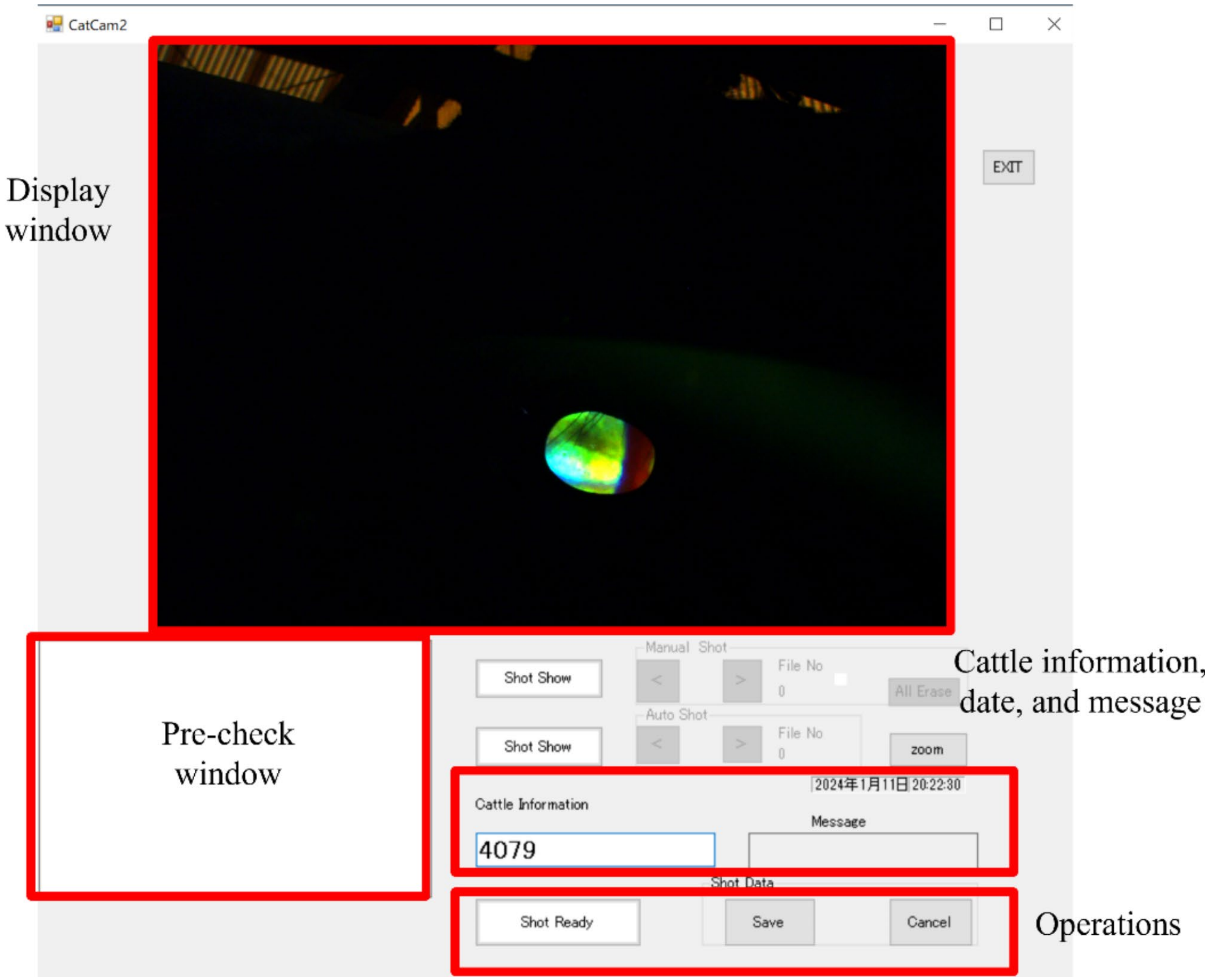

Fig. 5. The user interface in the fundus camera system. Functions like examining image quality, input of cattle ID, record for special conditions, as well as DNNs predictions can be performed.

	Han et al. 2018	Li et al. 2023		This study
Eye Image				
Class	Eye surface	Eye surface	Fundus	Fundus
Severe	0.62	-	-	0.87
Moderate	0.57	0.76	0.82	0.83
Mild	0.75			0.80

Table 5. Comparison of classification accuracy with previous studies.

site somewhat limited its widespread use. Moreover, they all need additional image processing procedure and cannot achieve real-time monitoring. The advancement of this research lies in the development of a handheld fundus camera system with DNNs algorithms deployed, enabling real-time prediction of vitamin A deficiency based on fundus photography. This methodology achieved practically significant accuracy, with averaged overall classification rates of 87%, 83%, 80% for the severe, moderate, and mild classes, respectively. This result surpasses all previous research and strongly support the advantage of this method.

Unlike in humans, cattle fundus usually does not exhibit visible biomarker abnormalities[15], and thus disease diagnosis based on cattle fundus image is more challenging. However, colour change is the easiest possible information we can obtain from the fundus image. The grain-based diet throughout fattening stage diminished vitamin A concentration in bloodstream. This, in turn, influenced the generation of visual photopigments[15] in the retinoid cycle in cattle retina and consequently changed its colour.

A deep learning research is incomplete without addressing its black box issue. Studies so far only provide the class-discriminative and highly detailed heatmaps[43,45–47] to visualise the target areas for the interpretability of the detection results. For a further analysis, this study not only conducted the heatmap visualisation using LPR, but also extracted chromatic features out from those heatmap-highlighted ROIs and then used them to predict blood vitamin A deficiency states. This provided a new method to explore the visualising heatmap, especially in the colour-related tasks. It was found chromatic features can explain 70% of prediction accuracy of the fundus-based vitamin A prediction in this deep learning study. It is apparent the YOLO model must have "learnt" more knowledge from the fundus images than merely focusing on the chromatic information. The comparison between the YOLO and the SVM prediction proves this sufficiently.

In the sample data studied, inter-class and intra-class chromatic variation was found across the three vitamin A deficiency classes. An example of the continuously captured fundus images from one session is compared in supplementary material Fig. S5, with their extracted features listed in supplementary material Table S5. Since the two images were captured in one session, no significant differences were found in the 21 chromatic features extracted. But resultantly one of two images was misclassified. This is partially due to the image's similarity to another one that belongs the mild class and possibly due to more sophisticated features based on which the model inferred. This study can only explain from the chromatic point of view.

Recent studies have also discovered that the effect of vitamin A on beef marbling shifts conversely at different growth stages[48–50]. A lower level of vitamin a promotes IMF deposition during the fattening stage, whereas at an early age (before 8 mo), the higher level does (Supplementary material Fig. S1). The mechanism is quite complex, and a good understanding and monitoring of blood vitamin A condition across cattle growth is crucial to the whole cattle industry. Our methodology offers a good solution to it.

On the other hand, at present, wagyu farmers rely on their raising experience to assess whether a steer is vitamin A deficient or not. This is rather subjective. Clear symptoms may only become apparent and observable when irreversible health damage has already occurred, making timely intervention helpless. This camera system can effectively mitigate such risks by early detection of cattle vitamin A deficiency and give warnings. It eliminates the need for laborious blood sampling or expensive blood assay, using instead non-invasive eye photography. The general prediction accuracy for three deficiency states all surpassed 80% and, in particular, 87% for the severe class. This can greatly facilitate cattle vitamin A levels monitoring to prevent diseases and minimise the animal stress exerted. It represents a substantial step forward towards achieving a higher level of animal welfare in wagyu industry.

Considering the unbalanced sample number for three vitamin A deficiency levels, non-colour related augmentation was adopted in this study to enlarge the sample data in severe class and to improve the model's generalisation ability. The originally collected images were rotated at angles between 0 and 45 degree and consequently, the sample number reached 1640 images in the severe class to rival the moderate (1974) and mild (1616) classes. Likewise, a three-fold cross validation was implemented for the vitamin A deficiency classification and the mean results were presented in supplementary material table S5-1. It is apparent the augmentation method slightly improved the mean classification accuracy for the three vitamin A deficiency classes where the largest increment was found in the severe class. This is due to the fact that the model learnt 'enough' features from the severe class-images and was able to identify them even at rotated angles. Besides, the augmented severe class is four times in quantity that of un-augmented one and the samples had great chance to be present in the validation set so as to be correctly classified. A basic rotation of the fundus images does not contribute significantly to the classification accuracy because the features extracted from the same fundus at varied angles should not differ so much.

This study has several limitations. First of all, by far there is no diagnostic standard of cattle fundus in terms of colour or any other features. However, there is a general trend of decreasing blue ratio components and increasing red ratio components found in the vitamin A depletion process[19,24,51]. Currently we have set up a fundus database of wagyu cattle in an attempt for reference images of different vitamin A deficiency state. Secondly, the experiment was conducted to the "Japanese Black" wagyu cattle from all the fattening stages (from 8 to 32 mo), but it has not been validated on wagyu cattle offspring overseas, such as purebred (or crossbreed) wagyu in US or Australia. Considering the fact that even Angus and other breeds[9,49,52,53]also exhibit similar marbling condition under vitamin A administration, it is anticipated that these wagyu offspring should demonstrate a similar performance. From physiological point of view, their fundus colour changes are presumably the same if subject to vitamin A deficiency. Yet further investigation is needed to confirm this. Thirdly, for the interpretation of the fundus-based vitamin A prediction, we explained from the chromatic features' perspective. Consideration of properties like fundus patterns or shapes would make the prediction model too complicated to interpret. Nevertheless, we believe relevant study would shed new lights on this project. Fourthly, as for DNNs architecture, we only used the basic YOLO v5s model in this system. Prediction accuracy could be further improved if trained with higher version of YOLO[44,54] models, or other DNNs architecture, as proven on COCO and other datasets.

Conclusions

This paper presented an easy-use handheld camera system capable of fundus photography and real-time vitamin A prediction with practically meaningful accuracy. It demonstrated the DL's effectiveness in cattle fundi classification regardless of the absence of abnormality, as is difficult in human fundus images. It also exemplified a new method to utilise visualisation heatmap in the colour-related deep learning study. It can assist farmers and veterinarians in vitamin A monitoring and related disease prevention during cattle rearing. This system contributes significantly to improving animal welfare in wagyu industry as well as a higher standard of precision livestock management.

Data availability

Part of the experimental results are presented in Supplementary materials and Raw data is available on request at li.nanding@imau.edu.cn.

Received: 10 October 2024; Accepted: 2 January 2025
Published online: 03 February 2025

References

1. Motoyama, M., Sasaki, K. & Watanabe, A. Wagyu and the factors contributing to its beef quality: A Japanese industry overview. *Meat Sci.* **120**, 10–18 (2016).
2. McDowell, L. R. *Vitamins in Animal Nutrition: Comparative Aspects to Human Nutrition* (Elsevier, 2012).
3. Oka, A., Maruo, Y., Miki, T., Yamasaki, T. & Saito, T. Influence of vitamin A on the quality of beef from the Tajima strain of Japanese black cattle. *Meat Sci.* **48**, 159–167 (1998).
4. Peng, D. Q., Smith, S. B. & Lee, H. G. Vitamin A regulates intramuscular adipose tissue and muscle development: Promoting high-quality beef production. *J. Anim. Sci. Biotechnol.* **12**, 1–10 (2021).
5. Bryant, T. C. et al. Effect of dietary supplemental vitamin A concentration on performance, carcass merit, serum metabolites, and lipogenic enzyme activity in yearling beef steers. *J. Anim. Sci.* **88**, 1463–1478 (2010).
6. Kruk, Z. A. et al. Effects of vitamin A on growth performance and carcass quality in steers. *Livest. Sci.* **119**, 12–21 (2008).
7. Kruk, Z. A. et al. Vitamin A and marbling attributes: Intramuscular fat hyperplasia effects in cattle. *Meat Sci.* **137**, 139–146 (2018).
8. Yamada, T., Kamiya, M. & Higuchi, M. Fat depot-specific effects of body fat distribution and adipocyte size on intramuscular fat accumulation in Wagyu cattle. *Anim. Sci. J.* **91**, 1–8 (2020).
9. Peng, D. Q. et al. Effect of vitamin A restriction on carcass traits and blood metabolites in Korean native steers. *Anim. Prod. Sci.* **59**, 2138–2146 (2019).
10. Van Donkersgoed, J. & Clark, E. Blindness caused by hypovitaminosis A in feedlot cattle. *Can. Vet. J.* **29** (1988).
11. O'donoghue, J. G. *Vitamin A deficiency in beef cattle**.
12. Kubo, H., Hirose, T. & Takahira, N. Relationship between liver disposal and carcass performance and profits of fattening cattle. *Bull. Livest. Res. Inst. Toyama Prefect. Agric. For. Fish. Res. Cent.* **3**, 17–24 (2013).
13. Licata, A. et al. The role of vitamin deficiency in liver disease: To supplement or not supplement?. *Nutrients* **13**. https://doi.org/10.3390/nu13114014 (2021).
14. Shastak, Y. & Pelletier, W. Balancing vitamin A supply for cattle: A review of the current knowledge (2024).
15. Maggs, D., Miller, P. & Ofri, R. *Slatter's Fundamentals of Veterinary Ophthalmology* (Saunders Elsevier, 2008).
16. Morshedian, A. et al. Light-driven regeneration of cone visual pigments through a mechanism involving RGR opsin in Müller glial cells. *Neuron* **102**, 1172–1183 (2019).
17. Kaylor, J. J. et al. Blue light regenerates functional visual pigments in mammals through a retinyl-phospholipid intermediate. *Nat. Commun.* **8**, 1–9 (2017).
18. Dale, P. et al. *Neuroscience* (Sinauer Associates, 2008).
19. Zhou, Y. et al. Automated pupil image acquisition to estimate serum Vitamin A levels in cattle using pupil color analysis. In *1st Asian-Australasian Conference on Precision Pastures and Livestock Farming* vol. 1, 1–6 (2017).
20. Tanigawa, S. et al. The relationship between serum vitamin A level of Japanese black cattle and light reflection on the pupil. In *2011 IEEE/SICE International Symposium on System Integration, SII* vol. 2011 187–191 (2011). https://doi.org/10.1109/SII.2011.6147443
21. Han, S. et al. Classification of vitamin A deficiency levels by ocular changes in Japanese black cattle. *Biosyst. Eng.* **173**, 71–78 (2018).
22. Han, S. et al. Feasibility of pupillary light reflex analysis to identify vitamin A deficiency in Japanese black cattle. *Comput. Electron. Agric.* **108**, 80–86 (2014).
23. Takao, Y. et al. Correlation between serum vitamin A level and pupil color of beef cattle. In *2011 IEEE/SICE Int. Symp. Syst. Integr. SII* vol. 2011 182-186. https://doi.org/10.1109/SII.2011.6147442 (2011).
24. Li, N. et al. An automatic eye surface-fundus double imaging system for estimation of vitamin A levels in Japanese black cattle. *Comput. Electron. Agric.* **210** (2023).
25. Li, N. et al. Blood vitamin A level prediction in Japanese black cattle based on chromatic and dynamic eye features using double imaging system. *Biosyst. Eng.* **244**, 107–113 (2024).
26. Zaidi, S. S. A. et al. A survey of modern deep learning based object detection models (2021).
27. Simonyan, K. & Zisserman, A. Very deep convolutional networks for large-scale image recognition (2014).
28. Dede, S., Vrochidou, E., Kanakaris, V. & Papakostas, G. A. Deep learning for cattle face identification. 316–335. https://doi.org/10.1007/978-3-031-66705-3_21 (2024).
29. Fang, C., Zhang, T., Zheng, H., Huang, J. & Cuan, K. Pose estimation and behavior classification of broiler chickens based on deep neural networks. *Comput. Electron. Agric.* **180**, 105863 (2021).
30. Milea, D. et al. Artificial Intelligence to detect Papilledema from Ocular Fundus photographs. *N. Engl. J. Med.* **382**, 1687–1695 (2020).
31. Goutam, B., Hashmi, M. F., Geem, Z. W. & Bokde, N. D. A Comprehensive review of deep learning strategies in retinal disease diagnosis using fundus images. *IEEE Access* **10**, 57796–57823. https://doi.org/10.1109/ACCESS.2022.3178372 (2022).
32. Cen, L. P. et al. Automatic detection of 39 fundus diseases and conditions in retinal photographs using deep neural networks. *Nat. Commun.* **12**, 1–13 (2021).
33. Wang, J. et al. Automated explainable multidimensional deep learning platform of retinal images for retinopathy of prematurity screening. *JAMA Netw. Open.* **4** (2021).
34. Wilkinson, C. P. et al. Proposed international clinical diabetic retinopathy and diabetic macular edema disease severity scales. *Ophthalmology* **110**, 1677–1682 (2003).
35. Gulshan, V. et al. Development and validation of a deep learning algorithm for detection of diabetic retinopathy in retinal fundus photographs. *JAMA - J. Am. Med. Assoc.* **316**, 2402–2410 (2016).
36. Sahlsten, J. et al. Deep learning fundus image analysis for diabetic retinopathy and macular edema grading. *Sci. Rep.* **9** (2019).
37. Christopher, M. et al. Performance of deep learning architectures and transfer learning for detecting glaucomatous optic neuropathy in fundus photographs. *Sci. Rep.* **8**, (2018).
38. Orlando, J. I. et al. REFUGE challenge: A unified framework for evaluating automated methods for glaucoma assessment from fundus photographs (2019). https://refuge.grand-challenge.org
39. Bach, S. et al. On pixel-wise explanations for non-linear classifier decisions by layer-wise relevance propagation. *PLoS One* **10** (2015).
40. Binder, A., Montavon, G., Bach, S., Müller, K. R. & Samek, W. Layer-wise relevance propagation for neural networks with local renormalization layers (2016).
41. Bykov, K., Hedström, A., Nakajima, S. & Höhne, M-C. M. *NoiseGrad — Enhancing Explanations by Introducing Stochasticity to Model Weights*. www.aaai.org (2022).
42. Selvaraju, R. R. et al. Grad-CAM: Visual explanations from deep networks via gradient-based localization. *Int. J. Comput. Vis.* **128**, 336–359 (2020).

43. Chen, L., Chen, J., Hajimirsadeghi, H. & Mori, G. Adapting grad-CAM for embedding networks (2020).
44. Jocher, G. YOLOv5 by Ultralytics (Version 7.0) (2020).
45. Karasmanoglou, A., Antonakakis, M. & Zervakis, M. Heatmap-based explanation of YOLOv5 object detection with layer-wise relevance propagation. In *IST 2022 - IEEE International Conference on Imaging Systems and Techniques, Proceedings (*Institute of Electrical and Electronics Engineers Inc., 2022). https://doi.org/10.1109/IST55454.2022.9827744
46. Selvaraju, R. R. et al. Grad-CAM: Visual explanations from deep networks via gradient-based localization. http://gradcam.cloudcv.org
47. Zhou, B., Khosla, A., Lapedriza, A., Oliva, A. & Torralba, A. Learning deep features for discriminative localization. http://cnnlocalization.csail.mit.edu
48. Yu, X. et al. Neonatal vitamin A administration increases intramuscular fat by promoting angiogenesis and preadipocyte formation. *Meat Sci.* **191**, 108847 (2022).
49. Harris, C. L. et al. Vitamin A administration at birth promotes calf growth and intramuscular fat development in Angus beef cattle. *J. Anim. Sci. Biotechnol.* **9**, 55 (2018).
50. Maciel, F. C. et al. Effect of vitamin A injection at birth on intramuscular fat development and meat quality in beef cattle. *Meat Sci.* **184**, 108676 (2022).
51. Han, S. et al. Estimation of serum vitamin A level by color change of pupil in Japanese black cattle. *Eng. Agric. Environ. Food* **6**, 177–183 (2013).
52. May, S. G. et al. Evidence for preadipocyte proliferation during culture of subcutaneous and intramuscular adipose tissues from Angus and Wagyu crossbred steers. *J. Anim. Sci.* **72**, 3110–3117 (1994).
53. Siebert, B. D. et al. Effect of low vitamin A status on fat deposition and fatty acid desaturation in beef cattle. *Lipids* **41**, 365–370 (2006).
54. Jocher, G., Chaurasia, A. & Qiu, J. Ultralytics YOLO (Version 8.0.0). *[Computer software]* (2023). https://github.com/ultralytics/ultralytics

Acknowledgements
Authors want to thank Takehiko Ohmae and Norio Nishiki for assistance in cattle management. We are grateful to Professor Garry John Piller (Graduate School of Agriculture, Kyoto University, Japan) for English proof reading. The author also greatly appreciates CSC (Chinese Scholarship Counsel) for scholarship.

Author contributions
N. L. did the experiment and formal analysis, and wrote the manuscript. N. K. Conceptualized the study and administered the project as well as funding. Y. O., K. S., and T. F. validated the results. M. S. assisted in the experiment.D. P. and N. S. helped with methodology.M. F. assisted in the experiment and methodology. X. D. reviewed the manuscript and edited.T. S. reviewed the writing and supervised the research.

Funding
This work was supported by KAKENHI [Grant Number 17H01500, 20H00439, 23H00350] from Japan Society for the Promotion of Science.

Declarations

Competing interests
The authors declare no competing interests.

Informed consent
Subjects appeared on the Fig. 2 are directly involved in this study, and are all informed about the publication of the identifying image/information in an online open-access publication.

Additional information
Supplementary Information The online version contains supplementary material available at https://doi.org/10.1038/s41598-025-85372-w.

Correspondence and requests for materials should be addressed to X.D. or T.S.